Electronic and atomic structure of the Cu/Si(111) quasi-5×5 overlayer

D. D. Chambliss* and T. N. Rhodin

School of Applied and Engineering Physics, Cornell University, Ithaca, New York 14853
(Received 1 March 1990)

The quasi-5×5 layer formed by annealing a monolayer of Cu on a Si(111) surface has a so-called quasiperiodic structure that differs significantly from both transition-metal silicides and metal-induced reconstructions. We have therefore performed detailed angle-resolved uv photoemission (ARUPS) measurements and *ab initio* band-structure calculations to investigate the atomic structure of the quasi-5×5 layer and the unique bonding behavior it embodies. ARUPS results are dominated by two Cu $3d$ peaks separated by 0.7 eV. The intensity variation of these peaks with emission and incidence angles suggests an ordered planar layer, yet there is considerable inhomogeneous broadening. A Si $3p$-derived surface state is also observed 1.2 eV below the Fermi level. Two atomic models are considered in light of these results: a widely cited nearly planar $CuSi_2$ model with interstitial Cu atoms and a substitutional CuSi model. In electronic-structure calculations using the pseudofunction method of Kasowski *et al.*, the CuSi model agrees much better than the $CuSi_2$ model with ARUPS in the energy differences between Cu $3d$ states, in their energies relative to the Fermi level, and in the surface-state behavior. Computed results for the CuSi model also account for features seen in current-voltage relationships in scanning tunneling microscopy, the Cu atom height measured with x-ray standing waves, the observed nonreactivity of the quasi-5×5 surface, and a vibrational mode at 8 meV detected using helium diffraction. The band-structure calculations show that bonding in the "5×5" CuSi layer is different from that of transition-metal silicides. The formation of Si p–Cu d bonding hybrid orbitals appears to be important in making the CuSi structure stable, but the Cu $4s$ orbitals also play a significant role in hybridizing with Si $3p$ states. It is possible that the quasi-5×5 layer is a two-dimensional electron phase in which domain boundaries are formed to accommodate a particular [Cu]:[Si] surface stoichiometry different from unity.

I. INTRODUCTION

The bonding behavior of noble metals on silicon crystals tends to be complex. Unlike most transition metals, a noble metal does not tend toward the formation of a covalently bonded bulk silicide whose structure dominates the surface reactions. In particular, the quasi-5×5 structure formed upon annealing monolayer quantities of Cu on Si(111) to 600 °C has an unusual and incompletely understood structure. The low-energy electron diffraction (LEED) pattern (Fig. 1) has spot positions suggestive of a (5×5) reconstruction, but accurate measurements of the uneven spot spacing[1] indicate that it has neither a (5×5) nor a (6×6) periodicity. This has been interpreted as indicating an incommensurate overlayer expanded or contracted by roughly 20%,[2] which suggests that overlayer-substrate interactions are relatively weak. Scanning tunneling microscopy (STM),[3,4] on the other hand, reveals a more complicated structure. There are regions with a hexagonal array of spots apparently commensurate with the Si(111) lattice. These regions are broken up by a quasiperiodic array of features that register with the hexagonal lattice, with a spacing that varies between five and seven lattice units. This quasiperiodic array accounts for the LEED pattern.[4] It is not clear what atomic structure underlies the STM images nor why a locally commensurate structure would be broken up into fairly well-ordered small domains. A helium-diffraction study,[5] shows that,

while there is medium-range disorder in the sense that spacing between adjacent features is variable, there are correlations among these spacings that correspond to a high degree of long-range order. The helium-diffraction results also indicate that the diffraction peak from the (1×1) part of the corrugation corresponds to periodicity *exactly commensurate* with the Si(111) substrate.
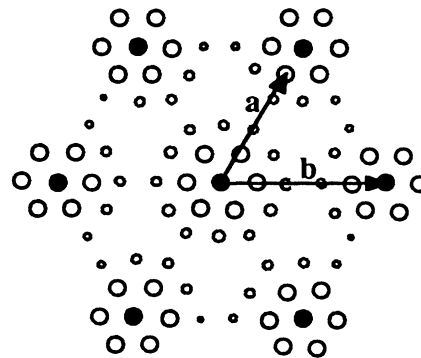

FIG. 1. Schematic representation of quasi-5×5 LEED pattern of annealed Cu on Si(111). Solid circles are (1×1) spots of substrate; overlayer spots are shown as open circles. Smaller circles denote much weaker spots that are not always visible, and other weak spots may also be visible. Actual spacing is uneven; Kemmann *et al.* report a/b =0.816±0.003 (Ref. 10).

Reflection electron micrographs[6] show that development of the quasi-5×5 structure proceeds by the growth of islands, as is illustrated schematically in Fig. 2. No distinct low-coverage structures have been reported, in contrast with the $(\sqrt{3}\times\sqrt{3})R\,30°$ structures induced by many metals on Si(111).[7] The islands with quasi-5×5 structure nucleate at bilayer steps and grow *at the same level* on both upper and lower terraces. The growth mode indicates that the islands are not pure Cu islands atop a Si substrate, for such islands should preserve the original step structure of the surface. Instead, island formation involves transport of Si from the upper to the lower terraces.[6] By measuring the ratio of areas between the portions of the quasi-5×5 islands over the upper and lower terraces, and using the amount of Si in the outer layers of the initial Si(111)-(7×7) structure,[8] the amount of silicon in the quasi-5×5 structure can be determined. If the quasi-5×5 structure is assumed to be a mixed Cu-Si layer above a complete Si bilayer, the mixed layer contains 1.33 ± 0.1 monolayer (ML) of silicon.[9] If the underlying bilayer has holes or intersitial Si, then the overlayer Si content would be correspondingly increased or decreased.

The copper content of the quasi-5×5 overlayer is indicated to be roughly 1.3 ML by a breakpoint in the graph of Auger peak height versus Cu coverage.[2] Kemmann et al.[10] measured slightly different breakpoints for samples not annealed to high temperature but heated during deposition: 1 ML for a substrate at 200 °C and 1.25 ML at 130 °C. Thermal-desorption measurements[10] suggest that the complete overlayer contains between 0.9 and 1.3 ML Cu. Thus it appears that the area-averaged stoichiometry of the quasi-5×5 layer is [Cu]:[Si] $=1:1.2\pm0.2$. The roughly equal amounts of Cu and Si would be consistent with a CuSi structure for the (1×1)

corrugated regions in scanning tunneling micrographs, possibly contracted to explain coverages greater than 1 ML. However, these results deal only with the area-averaged content of the surface and give no indication of local atomic structure. Indeed, this stoichiometry would be consistent with alternating regions of pure Cu and pure Si, though such a model is very unrealistic for other reasons.

The Auger-electron-diffraction study by Chambers et al. found that most Cu atoms are in roughly the outermost plane of the structure and that the emission has sixfold-azimuthal symmetry.[11] The Si(111) substrate, in contrast, has a threefold axis. To account for the increased symmetry, a model was proposed in which Cu atoms enter the hollow sites of an ideal Si(111) bilayer and the resulting $CuSi_2$ layer becomes planar. On the basis of comparison between experimental results and calculations, it was claimed that the Cu atoms lie 0.1 Å below the outer plane of Si atoms. These conclusions are limited, however, by the assumptions that all Cu sites are identical and that the structure is commensurate with the Si(111) substrate. The sixfold symmetry, however, could equally well result from the superposition of emission from inequivalent sites with lower symmetry such as, for example, two domain types with threefold symmetry.

The quasi-5×5 layer is not very chemically reactive; electron-energy-loss spectroscopy studies show that exposure to 10^4 L (1 L$=10^{-6}$ Torr s) of O_2 produces no significant Si oxidation[2] and that Si—H bonds are not formed when the quasi-5×5 layer is exposed to molecular hydrogen.[12] This indicates that Si atoms at the surface do not have dangling bonds.[12] The relatively small surface corrugation observed using STM shows that the dimer and adatom configurations that reduce the number of dangling bonds on clean Si surfaces are not present.

On the basis of the previous studies, two atomic models seem most likely for the dominant (1×1) regions of the quasi-5×5 overlayer. Auger-electron diffraction indicates a planar layer; this could be a CuSi substitutional structure [Fig. 3(a)] as favored by these authors and suggested by stoichiometry results, or a $CuSi_2$ interstitial-like structure [Fig. 3(b)] as suggested by Chambers et al.[11] The valence bands of a solid are quite sensitive to local
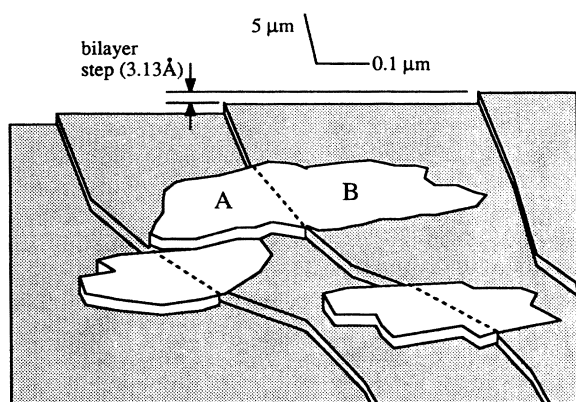

FIG. 2. Island structure of partial quasi-5×5 surface. Figure is based on reflection-electron-microscopy images (Ref. 6). Light patches are reacted Cu-Si islands, which grow in both directions from bilayer steps, approximately at the height of upper plateaus. Bilayer steps are not imaged directly, but are seen as Moiré fringes. Difference in length scale between width and depth is due to foreshortening. Fractions of island area above lower plateau (A) and at upper plateau (B) are measured to infer Cu-Si layer composition.
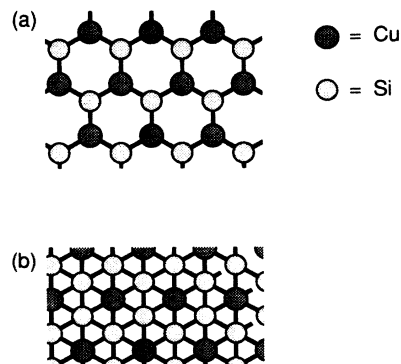

FIG. 3. Likely planar models for the quasi-5×5 structure. (a) CuSi layer, in plan view. (b) $CuSi_2$ layer.

structure, so angle-resolved uv photoemission (ARUPS) is a natural tool for choosing between these structures. The ordering of the Cu $3d$ states of different symmetry is a test of the planar Cu—Si bonding in these models, and the Cu $3d$ energies are sensitive to the difference between threefold bonding in the CuSi model and sixfold bonding in the $CuSi_2$ model. With band-structure calculations it is possible to determine which overlayer structure best explains the photoemission results. This information about local structure complements probes that are sensitive to longer-range structure, such as STM and helium diffraction.

II. EXPERIMENTAL PROCEDURES

The experiments were performed using a modified Vacuum Generators ADES-400 system, with a base pressure of 7×10^{-11} Torr, equipped with low-energy electron diffraction (LEED) optics and a single-pass cylindrical-mirror analyzer (CMA) for Auger-electron spectroscopy. Photoemission experiments used synchrotron radiation from the Tantalus I storage ring of the University of Wisconsin–Madison, in the photon-energy range 10–30 eV. The monochromator slits and the pass energy of the hemispherical electron analyzer were chosen to yield a combined resolution of 0.2 eV full width at half maximum, determined from the Fermi-edge cutoff for samples with heavy Cu deposits.

Photoemission experiments were performed on annealed layers of Cu on Si(111) substrates. The substrates were cut from a lightly doped p-type commercial Si(111) wafer, and were cleaned by cycles of Ar-ion sputtering and annealing to 900 °C by resistive heating to obtain sharp, strong (7×7) LEED patterns. Sample temperature was monitored both with a Chromel-Alumel thermocouple, which was attached to tantalum foil in contact with the sample, and with an infrared pyrometer. Cu was deposited at 1–2 monolayer (ML) per minute from a tungsten wire wrapped with 99.999%-pure Cu wire. Nominal Cu exposures were determined by measuring the evaporation rate with a quartz-crystal-thickness monitor before each evaporation. During evaporation the chamber pressure rose by approximately 2×10^{-10} Torr. Samples were prepared both by deposition onto a substrate at room temperature, followed by annealing to 600 °C, and by deposition onto a substrate held at 600 °C; the LEED patterns and photoemission results from samples prepared in these two ways did not differ significantly.

III. RESULTS OF ANGLE-RESOLVED PHOTOEMISSION

Angle-resolved-photoemission results are seen in Fig. 4 for three samples: a clean Si(111)-(7×7) surface; a "half-layer" sample with 0.6 ML Cu (nominal), annealed to 600 °C, which displayed both (7×7) and quasi-5×5 LEED spots; and a "full-layer" sample with 1.1 ML Cu (nominal), annealed, whose LEED pattern was pure quasi-5×5. At this photon energy (22 eV) the photoionization cross section of Cu $3d$ states is greater than that of Si $3p$, Si $3s$, and Cu $4s$ states,[13] so the dominant feature
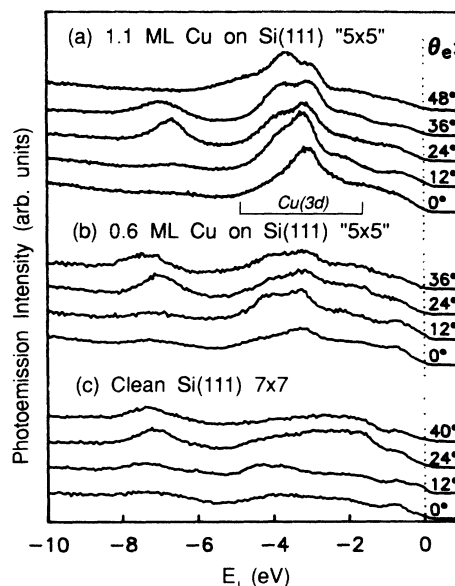

FIG. 4. ARUPS spectra from Cu/Si(111)-(quasi-5×5) at photon energy 22 eV at different emission angles in (Ī10) mirror plane. (a) "Full-layer" sample (1.1 ML Cu). (b) "Half-layer" sample (0.45 ML Cu). (c) Clean Si(111)-(7×7). Cu $3d$ region is labeled. Peaks near -7 eV are attributable to bulk transitions.

is the manifold of Cu $3d$-derived states that appears between -2.5 and -4.5 eV binding energy. Features due to Si bulk states also appear, most noticeably around -7 eV for emission angles around 30°. The shoulder around -5 eV for the topmost curve is also a bulk feature.

Spectra from the half- and full-layer samples are similar in peak energies and differ mainly in the amplitude of the Cu $3d$ emission. This suggests that annealed layers with different Cu coverages are composed of islands that have the same internal structure but cover different fractions of the surface. Increasing Cu coverage also increases the work function Φ, which causes bulk-state peaks to shift toward E_F. The peak in the "full-layer" spectra is shifted compared with Si(111)-(7×7) by 0.4 eV, because its work function is increased by 0.4 eV. Work functions of other samples were measured by subtracting the total width of the photoemission spectra from the photon energy. These results suggest that Φ of a completed quasi-5×5 layer is closer to 5.3 eV, which is 0.6 eV greater than that of Si(111)-(7×7). (The "full-layer" sample therefore may not have been completely covered with the quasi-5×5 layer.)

The Cu $3d$ manifold can be well described as the superposition of three peaks. These peaks, much broader than the instrumental resolution of 0.2 eV, are fitted well by Gaussian peaks with a full width at half maximum of about 0.7 eV. The Gaussian form suggests inhomogeneous broadening, which is expected given the structural variability seen in scanning tunneling micrographs. The peaks at normal emission are determined using photon polarization to be two states of Λ_3 symmetry at -3.1 and about -3.8 eV and one of Λ_1 symmetry at -2.5 eV. (The Λ_1 state does not appear as a peak in Fig. 4 because of Si bulk states at nearby energies, but it is clear in the

difference between spectra at different angles of incidence.) The near-disappearance of the lower Λ_3 state as normal emission is approached identifies this as a $d_{x^2-y^2}$ state and suggests that the Cu sites deviate only slightly from having C_{6v} or D_{3h} symmetry. Its nonzero intensity at normal emission suggests some mixing of states at $\bar{\Gamma}$ (i.e., breaking of the high symmetry), but is too weak to permit its energy to be determined accurately in the presence of the background intensity. The value -3.8 eV is measured for peaks at off-normal-emission angles with $k_{\parallel} = \bar{\Gamma}'$ equivalent to $\bar{\Gamma}$ by *umklapp*. The absence of true periodicity in the layer, demonstrated by scanning tunneling microscopy and inhomogeneous broadening in photoemission, means that the photoemission peaks are due to a number of related states, and dispersion of bands with $k_{\parallel}$ is not strictly applicable. It is still useful to measure the energy variation of peak maxima with emission angle and to treat it as if it is band dispersion, remembering the effect of disorder on this comparison. The measured dispersion of peak maxima with emission angle is shown in Fig. 5 as a function of $k_{\parallel}$.

At lower photon energies the photoionization cross section for Cu $3d$ becomes markedly lower, so the spectra primarily indicate Si states. The spectra in Fig. 6 were collected from a sample with a saturated quasi-5×5 overlayer grown by depositing 4.5 ML Cu at room temperature and annealing at 600 °C. This high Cu coverage used here ensures that the quasi-5×5 layer is complete. Excess Cu has been shown under these conditions to evaporate, leaving three-dimensional (3D) islands of Si that apparently had been dissolved in the initial Cu layer.[14] In this case the islands cause the LEED pattern to be less sharp than those from samples with less Cu deposition, but the characteristic "5×5" pattern remains. Comparisons at various photon energies indicate that the surfaces of these islands did not contribute significantly to the photoemission spectra. Most of the features in Fig. 6 are identified as bulk states in the underlying Si.[15] In addi-

FIG. 6. ARUPS spectra from saturated quasi-5×5 overlayer at $h\nu = 14$ eV. Emission is in the $(\bar{1}10)$ mirror plane, in an even-parity geometry. Most features reflect dispersion of bulk states, but the state near E_F that is marked is a surface state.

tion, a dispersive feature with minimum energy -1.2 eV is seen at emission angles around 40°, which corresponds to the boundary of the surface Brillouin zone. This state is a surface state 0.4 eV above the projected bulk-band maximum at this $k_{\parallel}$, which originates in a bulk state of L_3 symmetry.[16] The surface state appears to be split off from the bulk band by the different bonding environment for Si in or near the overlayer. The dispersion of this state, measured at several photon energies, is shown in Fig. 7.
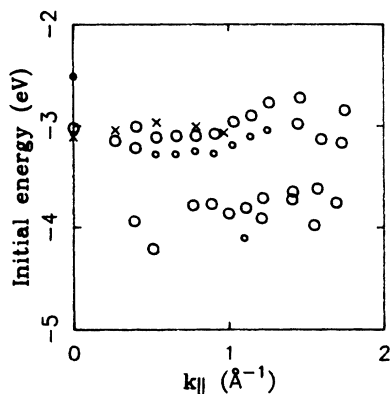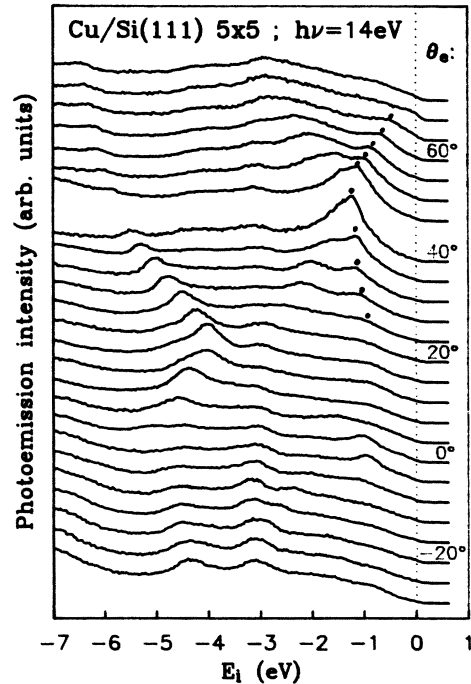

FIG. 5. Dispersion with parallel wave vector of Cu $3d$ peaks measured for quasi-5×5 layer with ARUPS at 22 eV photon energy. Circles are from spectra sensitive to even-parity states [vector potential $\mathbf{A}$ in the $(\bar{1}10)$ plane]. Crosses are from odd-parity spectra [$\mathbf{A}$ perpendicular to the $(\bar{1}10)$ plane]. Large circles are strong peaks, while small circles are shoulders with large uncertainty in energy.
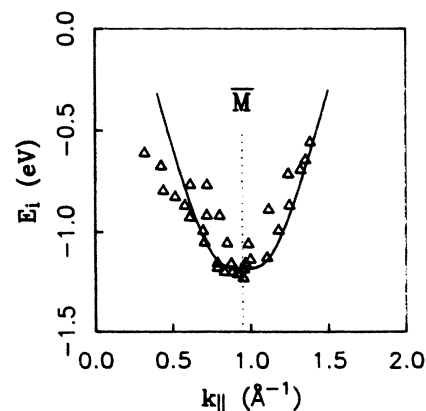

FIG. 7. Dispersion of surface state seen in spectra of Fig. 6. Peak energies were measured at various photon energies and emission angles.

The photoemission results by themselves indicate that the strongest interactions of the Cu atoms are with in-plane neighbors, for this gives rise to the observed ordering of the Cu $3d$ state energies ($d_{x^2-y^2}$ lowest). This agrees with the planar models that have been proposed. More specific structural conclusions utilize a detailed comparison of peak energies with calculated band structure for different models.

IV. CALCULATIONS: METHODS AND RESULTS

The electronic structure for several model atomic structures was computed within the local-density approximation (LDA) using the pseudofunction method developed by Kasowski et al.[17] The atomic models used for the calculations had (1×1) periodicity; they were not intended to represent the long-range structure of the quasi-5×5 Cu/Si layer, but, instead, to reproduce the essential features of local bonding. Experimental results are compared with computed dispersions for two different types of models. *Isolated layers* are models such as those shown in Fig. 3 in which no Si substrate is present. These models are useful for preliminary comparisons and for examining the systematic dependence of the Cu $3d$ energy separation on bond topology and on lattice constant. These models obviously do not represent overlayer-substrate bonding, and, in particular, include physically unrealistic dangling bonds that pin the Fermi level E_F, so these calculations cannot yield energy values relative to E_F. For such comparisons the more complete *double-sided slabs* shown in Fig. 8 are used; these consist of two Cu-Si mixed layers with one or two Si bilayers between, to represent bonding to the substrate. Our models representing the $CuSi_2$ model for the quasi-5×5 layer bonded to the substrate did not use a planar geometry, since it is unrealistic that Si atoms bonded to the sub-

strate would lie at the same level as those above hollow sites. Instead, the models used the structure of a Si bilayer with Cu added at different levels. The results discussed here did not depend much on the z positions chosen for the overlayer atoms. In particular, the energy structure of the Cu $3d$ states for a $CuSi_2$ model on a substrate was very similar to that for an isolated coplanar $CuSi_2$ layer. This was also true of computed results for CuSi layers.

The pseudofunction method has proved effective in computations on a range of problems, including bulk and surface properties of semiconductors.[17,18] The basis functions used in the pseudofunction method are similar to muffin-tin orbitals, but allow for a flexible choice of radial functions. The radial functions used here included sections of the true radial solution to the spherical potential derived in the self-consistent loop. Thus the basis functions respond directly to changes in the potential-energy function, even outside the muffin-tin spheres. The basis set included seven functions per Si atom ($3s$ and $3p^3$ states plus three higher-energy p functions to increase the variational freedom) and 16 functions per Cu atom ($4s$ and $3d^5$ states plus higher-energy s, p, and d functions). The irreducible wedge of the two-dimensional Brillouin zone was sampled on an evenly spaced grid of 16 points. The Fourier expansions defining the pseudofunctions included all plane waves with energy < 10.6 Ry (1 Ry $= 13.605$ eV). Augmentation energies were chosen so that the logarithmic derivative of the wave function at the muffin-tin radius was slightly negative.

Comparison of experiment with calculation focuses on the relative energies of Cu $3d$ levels, since these are expected to be computed reliably in the pseudofunction method. The isolated-layer calculations indicate that the CuSi planar structure gives nearly correct values for these relative energies, while for a $CuSi_2$ structure the separations are too great. Calculations for double-sided slabs confirm these results and clearly show that discrepancies in the isolated-layer results can be attributed to the effect of overlayer-substrate bonding.
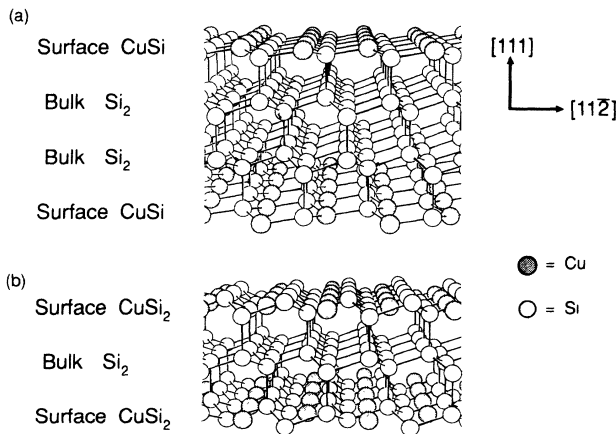
A. Comparison with calculated band structure for isolated layers

Calculated energy bands for isolated CuSi and $CuSi_2$ layers (Fig. 9) show the effect of bonding geometry on Cu $3d$ energy levels. For both, the Cu $3d$ states are concentrated at two energies, as is observed experimentally. At $\bar{\Gamma}$ in the surface Brillouin zone, the lower energy corresponds to $d_{x^2-y^2}$ and d_{xy} state (E' or E_{2g} representations, which correspond to the Λ_3 representation of the C_{3v} group of the [111] axis). At the higher energy are bands with Λ_3 symmetry (E'' and E_{1g}: d_{xz} and d_{yz} orbitals) and with Λ_1 symmetry (A'_1 and A_{1g}: d_{z^2}). For the CuSi layer the separation between the two d-state energies is about 0.8 eV, close to the experimental value of 0.7 eV. For a $CuSi_2$ layer the d-state behavior is qualitatively similar, but the d-state separation is much greater. Peak energies for different isolated-layer models are compared with experiment in Fig. 10. Isolated layers with different lattice constants are considered since the d-state splitting
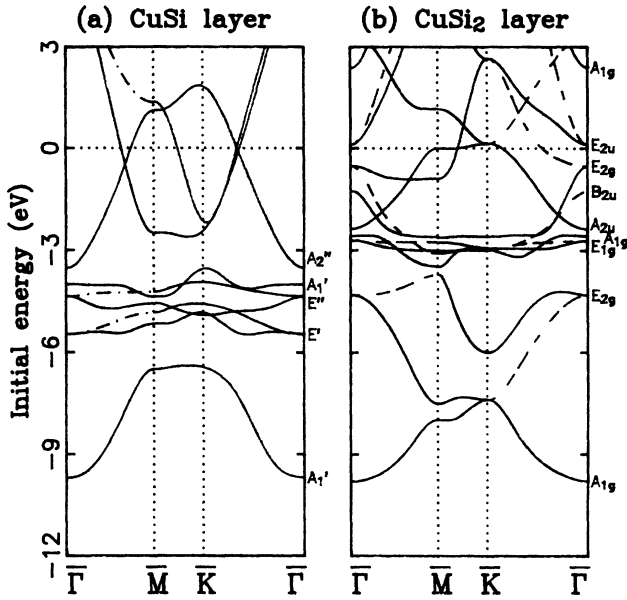

(a)
Surface CuSi
Bulk Si$_2$
Bulk Si$_2$
Surface CuSi

(b)
Surface CuSi$_2$
Bulk Si$_2$
Surface CuSi$_2$

◉ = Cu
○ = Si

FIG. 8. Double-sided models for electronic-structure calculations of Cu/Si(111)-(quasi-5×5). (a) Cu_2Si_6 unit cell model for CuSi overlayers. (b) Cu_2Si_6 unit-cell model for $CuSi_2$ overlayers. Models can be regarded as composed of stacks of bilayers and trilayers, as labeled. About 30 unit cells are viewed approximately along the [$\bar{1}$10] direction parallel to the surface. The actual model extends to $\pm \infty$ in x and y.

FIG. 9. Energy bands for single-layer coplanar models. (a) CuSi layer, contracted 20%. (b) CuSi$_2$ layer, expanded 20%. Line styles indicate parity with respect to mirror planes ($\bar{1}10$) for (a) and (b), and ($\bar{2}11$) for (b): solid lines, even parity; dashed lines, odd parity. Symmetry of $\bar{\Gamma}$ states is indicated at right for CuSi (D_{3h} symmetry) and CuSi$_2$ (D_{6h}). "A" and "B" parity representations correspond to the Λ_1 representation of the [111] axis symmetry, and "E" corresponds to Λ_3.
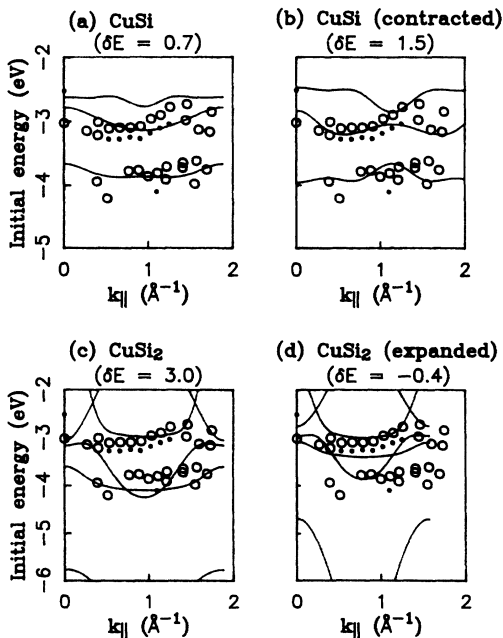

FIG. 10. Comparison of ARUPS results for even-parity states with calculated bands for isolated-layer models, along the line $\bar{\Gamma}$-$\bar{M}$-$\bar{\Gamma}$ in the surface Brillouin zone. Open circles are strong peaks and dots are shoulders. (a) CuSi commensurate layer. (b) CuSi layer, contracted 20%. (c) CuSi$_2$ layer. (d) CuSi$_2$ layer, expanded 20%. Computed bands are shifted in energy by δE values indicated.

depends sensitively on the Si-Cu internuclear distance as well as on the bonding topology, and structural probes have not unambiguously determined the overlayer lattice spacing. Since isolated-layer calculations do not relate surface levels to those of the bulk, the bands in each case are given a uniform energy offset δE chosen to improve agreement with the higher-energy Cu 3d states. [Since none of these models has a high density of states pinning the Fermi level, it is plausible that an energy shift of 1 V or more could arise from charge transfer when an isolated layer is attached to an ideal Si(111) surface.] The best agreement is for the contracted CuSi overlayer, represented in Fig. 10(b). The commensurate overlayer [Fig. 10(a)] also has bands concentrated at about the correct energies, although there is less agreement in the details of the dispersion. This difference between (a) and (b) is probably not significant because, as noted above, the observed ARUPS features are the aggregate of a number of similar bands. One discrepancy is that emission corresponding to the uppermost Cu 3d band, which contains mostly d_{z^2} states, is weak enough to be obscured by bulk emission. This is explained by strong hybridization with bulk states, as discussed below.

The CuSi$_2$-layer models show poor agreement with experiment [Figs. 10(c) and 10(d)]. In Fig. 10(c) the lower of the fairly flat bands appears to account for the lower-energy photoemission peaks, but at $\bar{\Gamma}$ it is a d_{xz} state and should produce a strong peak at normal emission, which is not seen. Furthermore, both models have $d_{x^2-y^2}$ states at $\bar{\Gamma}$ at low energies [-5.8 eV in (c), -4.7 eV in (d)]. While this should not be seen at normal emission, it should produce a strong peak for $k_\parallel$ at $\bar{\Gamma}'$ (around 1.6–1.8 Å^{-1}), which does not appear experimentally. Thus an isolated CuSi layer produces relatively good agreement with ARUPS results, while a CuSi$_2$ layer does not.

B. Comparison with calculated band structure for two-sided models

The effect of the Si substrate on the Cu/Si overlayer is calculated using two-sided models with Cu$_2$Si$_6$ unit cells and with a lattice constant equal to that of Si(111). The main conclusion drawn from the isolated-layer calculations is confirmed with the two-sided models: the Λ_3-state separation at $\bar{\Gamma}$ is correct for the CuSi model, but too large by a factor of 2 or 3 for a CuSi$_2$ model. The dispersion curves for the two-sided models (Fig. 11) do, however, reveal changes from the isolated-layer calculations. The Cu 3d bands for the two-sided models have more dispersion than those for the isolated layers, which does not agree with the fairly dispersionless behavior seen in photoemission. This difference between calculation and experiment is attributed to the lack of periodicity in the real system.

If the calculation were ideal, each Cu 3d state of the surface would appear as two degenerate bands, since the two surfaces containing Cu atoms should not affect each other. At $\bar{\Gamma}$, states with symmetry L_1 and L'_1 would be degenerate, as would states of L_3 and L'_3 symmetry. The

actual calculations, however, could only use fairly thin slabs as model structures. Although the two layers are far enough apart (> 6 Å) that the Cu $3d$ orbitals have negligible direct overlap, these orbitals do hybridize with Si orbitals to form states that do not completely decay across the thickness of the slab. The variation of this effect is an indicator of the sensitivity of particular states to substrate hybridization. In both CuSi and CuSi$_2$ geometries, the L_3 and L'_3 states at $\bar{\Gamma}$ are very nearly degenerate. The Cu $3d$ states are in a band gap of the bulk Si states that have Λ_3 symmetry, so they do not hybridize and penetrate the slab. In the CuSi model this continues from $\bar{\Gamma}$ to $\bar{M}$ for states of odd parity with respect to the mirror plane, so these four bands appear as only two curves in Fig. 11. On the other hand, the d_{z^2} levels at $\bar{\Gamma}$ (Λ_1 symmetry) are split by almost 1 eV in Fig. 11(a) and by over 2 eV in Fig. 11(b). This indicates strong hybridization with the bulk Si states. In a real overlayer this state would probably be a broad surface resonance. The

FIG. 11. Energy-band dispersion for models of the quasi-5×5 structure with a Si substrate. The surface structures are (a) CuSi and (b) CuSi$_2$. Cu $3d$ states are marked as follows: $\Diamond$, $d_{x^2-y^2}/d_{xy}$ character; $\triangle$, d_{xz}/d_{yz} character; $\bullet$, states at $\bar{\Gamma}$ with d_{z^2} character, split by substrate interaction. "S" marks surface states at $\bar{M}$ of the CuSi layer. Labels at right of each graph denote symmetry of states at $\bar{\Gamma}$. The notation is that used for L in the bulk Brillouin zone. (Point group D_{3d}: $1 = L_1 = A_g$; $1' = L'_1 = A_u$; $3 = L_3 = E_g$; $3' = L'_3 = E_u$.) The Λ_1 representation of the (111) axis symmetry contains both L_1 and L'_1, and the Λ_3 state contains both L_3 and L'_3. Solid and dashed lines denote even and odd parity, respectively. Along $\bar{\Gamma}$-$\bar{M}$, parity is with respect to ($\bar{1}10$) mirror plane of crystal. Along $\bar{M}$-$\bar{K}$ and $\bar{K}$-$\bar{\Gamma}$, parity is with respect to two different C_2 axes of the model which are not characteristic of the true surface.

d_{xz} and $d_{x^2-y^2}$ states at $\bar{\Gamma}$ are affected slightly by hybridization through the slab. While there is some splitting between states with different parity under inversion of the film, this artificial splitting is relatively small compared with the physically meaningful energy difference between d_{xz} and $d_{x^2-y^2}$ states.

Another effect of bonding to the substrate in both CuSi and CuSi$_2$ models is a slight increase in the separation between the states with Λ_3 symmetry. The substrate apparently satisfies the z-directed bond of the overlayer Si atoms, so that in-plane bonding with Cu atoms becomes more favorable. The separation between bonding and nonbonding Cu $3d$ orbitals is increased, and the layer is chemically more stable on a substrate than as an isolated layer.

The two-sided models do not involve any local bonding configurations that are not found in the ideal (i.e., semi-infinite) models, so the states determining the Fermi level should be represented accurately. Thus energies relative to the Fermi level are not subject to the distortion found in isolated monolayer models. For the commensurate CuSi$_2$ model [Fig. 11(b)] the upper Cu $3d$ states are too deep by 3 eV. This is strong evidence against this model, which corresponds to the Chambers model of the quasi-5×5 surface. An *expanded* CuSi$_2$ model might pass this test, however, because expanding the CuSi$_2$ layer moves the Cu $3d$ bands toward E_F. (This is reflected in the different δE values used in Fig. 10.) However, the absolute energies for the CuSi model are much closer to the experimental values, and the remaining difference of 0.35 eV could be due to the effect of substrate bonding on an incommensurate layer or the uncertainties in comparing the calculations to photoemission (Sec. VI).

The bands in Fig. 11 explain the surface state seen in photoemission from the quasi-5×5 layer at 14 eV photon energy (Figs. 6 and 7). The CuSi model has a pair of states at $\bar{M}$, with energies -1.0 and -1.7 eV, whose charge density is concentrated at the surface Si atoms ["S" in Fig. 11(a)]. The 0.7-eV energy separation, due to hybridization through the thin slab, implies a relatively large error bar on the calculated surface-state energy. Within this uncertainty, the energy and dispersion from $\bar{M}$ toward $\bar{\Gamma}$ of the calculated state agrees with the photoemission results. It remains to be verified in calculations on thicker slabs that a discrete surface state at $\bar{M}$ is split from the continuum of bulklike states. Calculations on the CuSi$_2$ model, on the other hand, do not yield a state that appears to correspond to the observed surface state. This is not surprising since the Fermi level for this model differs clearly from experiment. There is an occupied surface state at -1 eV, but that state is a dangling bond with incorrect dispersion.

In summary, the calculations on double-sided model slabs reinforce the support for the CuSi model. It is notable that bonding to the substrate markedly changes the Cu $3d_{z^2}$ state, which represents the only important disagreement between experiment and calculation for an isolated CuSi layer. The d_{xz} and $d_{x^2-y^2}$ states at $\bar{\Gamma}$ are not greatly affected, so experimental agreement with calculated bands remains good for the CuSi model and poor
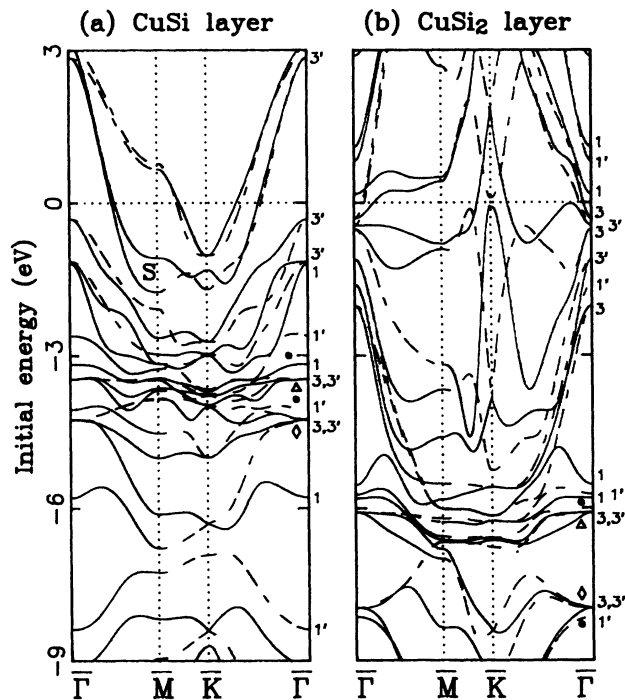
for the $CuSi_2$ model. The energies of states relative to the Fermi level, and the behavior of the surface state, are represented well by the CuSi model, and not by the $CuSi_2$ model. The discrepancies that remain are attributable to the complexity of the long-range structure of the real films, which could not be incorporated into the calculations at the start of the study.

C. Comparison to scanning tunneling microscopy

Calculated results were also used to simulate images produced using the scanning tunneling microscope (STM). Simulated images for several bias voltages were derived from the spatial variation of the local density of states.[19] It was found, however, that these simulated images were highly sensitive to small variations in atomic structure, so detailed comparison between simulated and experimental STM images would not be meaningful until the long-range structure is represented accurately in the calculations. The comparison of computations with STM results was done using band-structure diagrams and corresponding density-of-states results.

STM images of the Cu/Si(111)-(quasi-5×5) surface include regions of (1×1) corrugation. Topographic images do not indicate what atoms cause the observed features, but more information is found by measuring the tunnel current as a function of voltage with the tip at a fixed position. Such an STM I-V curve is shown in Fig. 12, collected with the tip at one of the high spots of the (1×1)
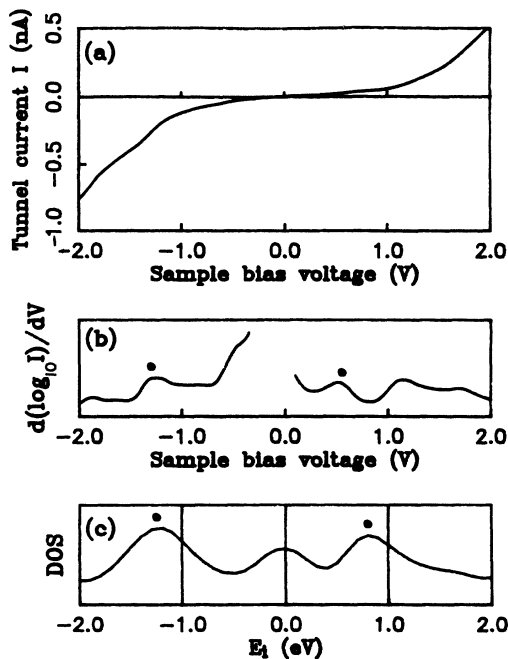

FIG. 12. Comparison of STM I-V measurement with band-structure calculations of commensurate CuSi layer on Si(111). (a) STM I-V data at high point of (1×1) corrugation. (b) Logarithmic derivative $d(\log_{10}I)/dV$ for data of (a). Peaks in this curve usually indicate DOS peaks. (c) Calculated local DOS at surface Si atom. STM data courtesy of U. Koehler, J. E. Demuth, and R. J. Hamers of IBM Research.

corrugation. Bias variation causes changes both in which states are energetically allowed to tunnel and in the tunneling rate of each allowed state. The latter effect causes the exponential variation seen in the high-bias portions of Fig. 12(a). The smaller variations in current at biases of -1.4 and $+0.7$ V, emphasized in the logarithmic derivative plot of Fig. 12(b), are probably caused by inclusion of new density-of-states (DOS) peaks in the range of allowed states. These features probably correspond to peaks in the computed local DOS at the surface Si in a CuSi layer on a Si substrate [Fig. 12(c)]. These peaks arise largely from the surface states near $\overline{M}$ in the surface Brillouin zone, one occupied and the other unoccupied. The occupied state is a Si $3p_z$ state concentrated directly above the surface Si atoms. The unoccupied state, on the other hand, is primarily of Si $3p_y$ character. The different character of these states accounts for the relative weakness of the experimental feature at $+0.7$ V: the occupied state projects outward from the surface and the unoccupied state does not. It should be noted that the feature at -1.4 V in the I-V curve is close to a DOS peak of bulk Si at the L_3 saddle point in the band. Thus the CuSi-layer model is not unique in predicting an STM I-V feature near this voltage.

D. Total-energy results

While the computations did not fully explore the variation of total energy between different atomic configurations, one particular set of results is worth noting. The variation in total energy of a CuSi overlayer with the Cu atom's displacement normal to the surface was calculated using a one-sided model consisting of a CuSi layer attached to a Si bilayer [i.e., half of the two-sided slab model shown in Fig. 8(a)]. The energy minimum is at 0.39 Å above the "coplanar" Si layer, or, equivalently, 3.13 Å above the center of the underlying Si bilayer. This position is relaxed inward somewhat from the position of the missing Si in the ideal bilayer, where a strictly substitutional Cu atom would reside. The calculated position is close to the x-ray-standing-wave experiments of Patel, which indicate that the average vertical position of the Cu atoms is 3.07 Å above the center of the underlying Si bilayer.[20]

A parabolic fit to the total-energy curve yields a force constant $\kappa = 2.5$ eV Å^{-2}±30%, which corresponds to a vibrational energy $\hbar\omega = 13\pm2$ meV. This motion of Cu atoms corresponds to a $q=0$ optical phonon of the hypothetical (1×1) CuSi overlayer, provided the constraint is imposed that all Si atoms remain fixed. This constraint causes an underestimate of the optical-phonon frequency, but the force constant for Si motion relative to the substrate (which stretches a Si—Si bond) should be much larger than for Cu motion relative to the coplanar Si (which mostly involves bond-angle distortion), so the discrepancy should not be large. If the calculations were extended to allow Cu atoms in neighboring unit cells to move in opposite directions, which would correspond to phonons with nonzero q, the restoring force per Cu atom should be lower than for in-phase motion because the bond-angle distortion of the Si atoms would be less.

Therefore the $q=0$ optical-phonon energy is probably an upper bound of the transverse vibrational energies of the hypothetical (1×1) overlayer. Inelastic-helium-scattering measurements have found a broad, flat energy-loss mode at 8 meV whose dispersionless character is attributed to the complex domain structure of the true overlayer and consequent localization of vibrational modes.[5] The energy is consistent with the behavior discussed above for vertical vibration of Cu, but more extensive calculations are needed to verify this assignment.

V. DISCUSSION AND CONCLUSIONS

The experimental evidence suggests that the quasi-5×5 structure consists largely of a planar overlayer that is at least locally well ordered. This is indicated by the dominance of two features with distinct angular momentum in the Cu $3d$ photoemission results, as well as by the amplitude of Auger-electron anisotropies and the (1×1) corrugation of STM images with which quasiperiodic features align. Of these experiments, only photoemission results give a reliable indication of the local chemical environment of the Cu atoms. These results indicate that the dominant part of the overlayer has CuSi composition.

In reviewing the conclusions from photoemission experiments and computational analysis, it is important to consider the accuracy to which the calculations can be expected to model photoemission results. There are three main sources of uncertainty: the local-density approximation (LDA), approximations intrinsic to the pseudofunction method, and the approximate nature of the atomic models used. The LDA is not rigorously valid for predicting photoemission results, but the magnitude of the error can be estimated. Energies of initial states in photoemission will have errors that depend on how localized the states are. For the quasi-5×5 overlayer, the Cu $3d$ states are not strongly hybridized with Si orbitals and are thus similar in their radial wave functions. Errors in *relative* energies of these states should therefore be small, although their energies relative to the Fermi level might be in error by a large fraction of an electron volt. We lack a calibration of photoemission versus the LDA for a copper-silicon system of known structure, but in the case of $CoSi_2$ it is found that the band structure computed using the linear augmented-plane-wave (LAPW) method[21] agrees within 0.2–0.4 eV with the energies of bonding and nonbonding peaks measured using photoemission.[22] The errors in relative $(3d)$ energies should be smaller in the Cu/Si case because the different metal $(3d)$ states differ less in their hybridization with silicon (sp) orbitals.

A similar argument applies to the uncertainty in the pseudofunction method. When the band structure of $CoSi_2$ computed using the pseudofunction method is compared with the LAPW results,[21] it is seen that the pseudofunction method overestimates the Co $3d$ bonding-nonbonding energy difference in $CoSi_2$ by 50%. The overestimate appears to be due to the incompleteness of the pseudofunction basis set. In the Cu-Si case the eigenstates with metal $3d$ character are much closer to

atomic orbitals than in $CoSi_2$, so the limited freedom of hybridization in the computational system should be less important. Thus the relative error in the energy difference should be somewhat less. For the Cu-Si calculations, with splittings of ~ 1 eV, the error in d-state differences is taken to be $(+15\%)/(-30\%)$.

The discrepancies between the $CuSi_2$ model and the photoemission results are well outside these error bounds. Thus this model does not represent the majority of the Cu/Si(111)-(quasi-5×5) layer. For a CuSi overlayer the agreement of theory with photoemission is much more convincing. Neither an isolated layer nor a commensurate layer on a substrate gives perfect agreement, but the discrepancies may be accounted for by the variability in the overlayer-substrate bonding configuration in the complex long-range structure.

The CuSi-layer model also explains the observed nonreactivity of the quasi-5×5 layer. Intuition suggests that the Si atoms of the $CuSi_2$ layer that are not bonded to the substrate would have an outward dangling bond, and this is confirmed by the calculations. In the CuSi model, on the other hand, the states near E_F are predominantly of p_x and p_y character. Thus the $CuSi_2$ layer should be fairly reactive, while the CuSi layer will be mostly inert, as is observed.

The conclusions about local bonding pertain to the majority of Cu atoms, and a minority (up to about 25%) might reside in different sites with, e.g., lower symmetry or higher coordination to Si atoms. This uncertainty is a consequence of the difficulty in identifying weak-photoemission structures in the presence of strong, broad peaks. The presence of variations in local atomic structure is suggested by the STM images. Furthermore, since the CuSi layer has only threefold symmetry, the presence of distinct domains is necessary to account for the sixfold symmetry observed with Auger-electron diffraction.[11] A determination of the domain boundary structure would be an important contribution to understanding the long-range structure of the quasi-5×5 layer. Nearest-neighbor distances determined using surface extended x-ray-absorption fine structure and particular multiple-scattering trajectories measured in hyperthermal ion-scattering experiments may be useful for identifying particular structures at domain boundaries.

One mechanism that could cause domain formation would be strain relief. In an overlayer with strong covalent bonding, the accumulation of lattice mismatch could cause the overlayer to reduce its strain energy by breaking up into somewhat irregular domains. The CuSi configuration favored in this study appears similar to covalently bonded structures formed by some p-electron metals on Si(111). This suggests that the directionality of silicon bonding induces Cu to behave almost like a p-electron metal. However, this accumulated-mismatch mechanism should involve some expansion or contraction of the (1×1) regions, in contradiction to helium-diffraction data.[5] Furthermore, this mechanism should not produce the long-range order seen with helium diffraction.

An interesting alternative to the strain-relief model is that the quasi-5×5 structure is a 2D electron phase. For

a given lattice parameter of the CuSi structure, there may be a particular density of electrons in delocalized Cu $4s$–Si $3p$ hybrid states at the surface that is energetically optimal. In this case there would be a driving force toward a particular Cu:Si stoichiometry that differs from unity, and domain boundaries might exist to accommodate, say, Cu enrichment that would yield the optimum density. This could explain the disorder at medium range (variability of domain size) and greater order at longer range observed with helium diffraction.[5] It is notable that the bulk alloy Cu_3Si is considered an electron phase[23] and has a complex long-range structure. The situation for Cu on Si(111) is more complicated than bulk Cu_3Si because of the strong constraints imposed by bonding to the Si(111) substrate. It may be fruitful to prepare CuSi overlayers on substrates with different lattice spacings [as by codeposition of Cu and Si on (111) faces of Ge_xSi_{1-x} crystals] to gain further insight into the nature of the quasi-5×5 structure on Si(111).

Note added in proof. It has been reported, on the basis of x-ray standing-wave and surface extended x-ray-absorption fine-structure experiments, that Cu/Si(111)-("5×5") has an expanded Cu_2Si structure [J. Zegenhagen, J. R. Patel, E. F. Fontes, and M. M. Marcus, Bull. Am. Phys. Soc. **35**, 451 (1990)]. This model was not examined in the present work and may be consistent with photoemission observations. The low Si content of such a layer (0.6–0.7 ML) implies that Si released from a growing Cu-Si island must be either incorporated into subsurface layers or transported away from the island (cf. Fig. 2 and accompanying discussion).

ACKNOWLEDGMENTS

*Present address: IBM Research Division, Almaden Research Center, 650 Harry Road, San Jose, CA 95120.

[1]E. Daugy, P. Mathiez, F. Salvan, and J. M. Layet, Surf. Sci. **152/153**, 1239 (1985).

[2]E. Daugy, P. Mathiez, F. Salvan, and J. M. Layet, Surf. Sci. **154**, 267 (1985).

[3]R. J. Wilson, S. Chiang, and F. Salvan, Phys. Rev. B **38**, 12 696 (1988).

[4]J. E. Demuth, U. Koehler, R. J. Hamers, and P. Kaplan, Phys. Rev. Lett. **62**, 641 (1989).

[5]R. B. Doak and D. B. Nguyen, Phys. Rev. B **40**, 1495 (1989).

[6]T. Ishitsuka, K. Takayanagi, Y. Tanishiro, and K. Yagi, in *Proceedings of the XIth Congress on Electron Microscopy* (Japanese Society of Electron Microscopy, Tokyo, 1986), p. 1347.

[7]See, e.g., T. Kinoshita, S. Kono, and T. Sagawa, Phys. Rev. B **34**, 3011 (1986).

[8]K. Takayanagi, Y. Tanishiro, M. Takahashi, and S. Takahashi, Surf. Sci. **164**, 367 (1985).

[9]D. D. Chambliss, Ph.D. thesis, Cornell University, 1989. More precisely, if the underlying bulk Si is taken to consist of ideal Si(111) bilayers, then there is an average of 1.33 ± 0.1 Si atoms outside the last bilayer per unit area defined by the Si(111)-1×1 unit cell. 1 ML as used here is the density of Si(111) surface atoms, 7.8×10^{14} cm^{-2}.

[10]H. Kemmann, F. Müller, and H. Neddermeyer, Surf. Sci. **192**, 11 (1987).

[11]S. A. Chambers, S. B. Anderson, and J. H. Weaver, Phys. Rev. B **32**, 581 (1985).

[12]S. A. Chambers, M. del Giudice, M. W. Ruckman, S. B. Anderson, J. H. Weaver, and G. J. Lapeyre, J. Vac. Sci. Technol. A **4**, 1595 (1986).

[13]J. J. Yeh and I. Lindau, At. Data Nucl. Data Tables **32**, 1 (1985).

[14]S. A. Chambers and J. H. Weaver, J. Vac. Sci. Technol. A **3**, 1929 (1985).

[15]For reference on ARUPS from Si(111)-(7×7), see R. I. G. Uhrberg, G. V. Hansson, U. O. Karlsson, J. M. Nicholls, P. E. S. Persson, S. A. Flodström, R. Engelhardt, and E.-E. Koch, Phys. Rev. B **31**, 3795 (1985).

[16]The experimental value of $E(L_3)$ is $E_{VBM}-1.6\pm0.1$ eV (Ref. 15). The work-function increase of 0.6 eV in going from Si(111)-7×7 to the quasi-5×5 layer puts $E_{VBM}\approx E_F$.

[17]R. V. Kasowski, T. N. Rhodin, M.-H. Tsai, and D. D. Chambliss, Phys. Rev. B **34**, 2656 (1986).

[18]M.-H. Tsai, R. V. Kasowski, and T. N. Rhodin, Surf. Sci. **179**, 143 (1987); M.-H. Tsai, J. D. Dow, and R. V. Kasowski, Phys. Rev. B **38**, 2176 (1988).

[19]J. Tersoff, M. J. Cardillo, and D. R. Hamann, Phys. Rev. B **32**, 5044 (1985); J. Tersoff, *ibid.* **39**, 1052 (1989).

[20]J. R. Patel (unpublished).

[21]L. F. Mattheiss and D. R. Hamann, Phys. Rev. B **37**, 10 623 (1988).

[22]G. Gewinner, C. Pirri, J. C. Peruchetti, D. Bolmont, J. Derrien, and P. Thiry, Phys. Rev. B **38**, 1879 (1988); D. D. Chambliss, T. N. Rhodin, and J. E. Rowe (unpublished).

[23]T. B. Massalski, in *Physical Metallurgy*, 3rd ed., edited by R. W. Cahn and P. Haasen (Elsevier, Amsterdam, 1983).
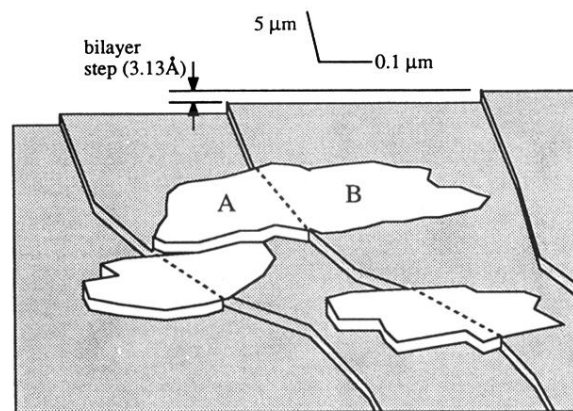
FIG. 2. Island structure of partial quasi-5×5 surface. Figure is based on reflection-electron-microscopy images (Ref. 6). Light patches are reacted Cu-Si islands, which grow in both directions from bilayer steps, approximately at the height of upper plateaus. Bilayer steps are not imaged directly, but are seen as Moiré fringes. Difference in length scale between width and depth is due to foreshortening. Fractions of island area above lower plateau (A) and at upper plateau (B) are measured to infer Cu-Si layer composition.

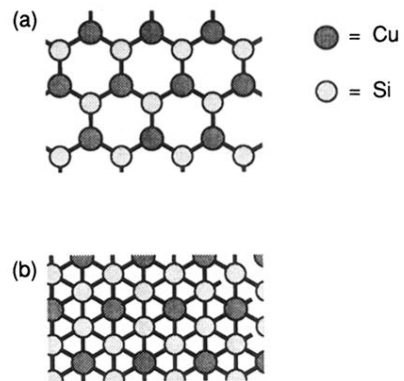FIG. 3. Likely planar models for the quasi-5×5 structure. (a) CuSi layer, in plan view. (b) CuSi$_2$ layer.
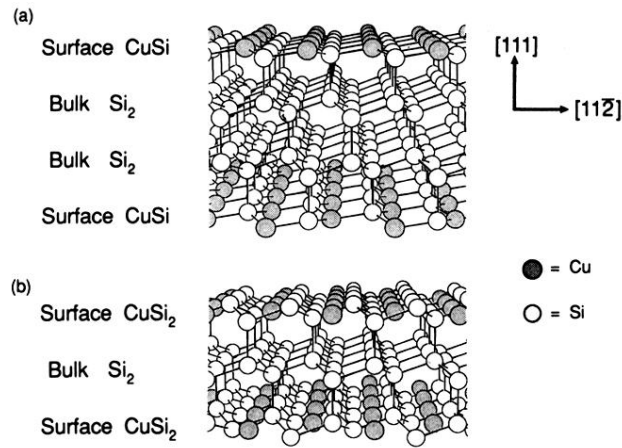
FIG. 8. Double-sided models for electronic-structure calculations of Cu/Si(111)-(quasi-5×5). (a) Cu_2Si_6 unit cell model for CuSi overlayers. (b) Cu_2Si_6 unit-cell model for $CuSi_2$ overlayers. Models can be regarded as composed of stacks of bilayers and trilayers, as labeled. About 30 unit cells are viewed approximately along the $[\bar{1}10]$ direction parallel to the surface. The actual model extends to $\pm\infty$ in x and y.